Syntheses, Structural Characterisation and Electronic Structures of Ferrocenyl-Osmafuran Heterobinuclear Organometallic Complexes

Bin Liu,*[,†,‡] Chun-Lan Guo,[†] Wen-Xia Liu,[†] Ming-E Guo,[†] Feng Yan,[†] Lu-Sha Xue,[†] Huijuan Wang,[§] Chang-Lin Liu,[†] Shan Jin,*[,†]

[†]*Key Laboratory of Pesticide and Chemical Biology, Ministry of Education, College of Chemistry, Central China Normal University, Wuhan 430079, P.R. China.*

[‡]*College of Chemistry & Chemical Engineering, Hubei University, Wuhan, 430062, P.R. China.*

[§]*Wuhan Institute of Physics and Mathematics, Chinese Academy of Sciences, Wuhan 430079, P.R. China.*

1. Crystallographic Information

Table S1. Crystal Data, Date Collection, and Refinement Parameters for **1**, **3**, and **4**.

Complex	**1**	**3**	**4**
Empirical formula	$C_{73}H_{68}Cl_6FeOOsP_3$	$C_{71}H_{59}Cl_4FeN_2OOsP_3S_2$	$C_{61.50}H_{58}Cl_7FeOOsP_3$
Formula weight	1512.93	1501.08	1400.19
T (K)	100(2)	100(2)	100(2)
Wavelength (Å)	0.71073	0.71073	0.71073
Crystal System	Monoclinic	Triclinic	Monoclinic
Space group	$P2_1/n$	*P*-1	$P2_1/n$
a (Å)	14.7133(10)	11.3898(19)	12.8226(8)
b (Å)	20.3718(13)	13.782(2)	21.1839(14)
c (Å)	23.0817(15)	22.283(4)	22.4869(15)
α (°)	90	95.356(2)	90

β (°)	103.2620	97.768(2)	103.8090(10)
γ (°)	90	111.383(2)	90
V (Å^3)	6733.9(8)	3188.5(9)	5931.6(7)
Z	4	2	4
F(000)	3052	1508	2804
D_{calcd} (Mg m^{-3})	1.492	1.564	1.568
μ (mm^{-1})	2.453	2.573	2.822
Reflection collected	11780	21708	62638
Unique Reflection	11780	11043	18739
R_{int}	0.0000	0.0359	0.0305
GOF	1.089	1.062	1.039
R_1 (I>2σ(I))	0.0378	0.0608	0.0374
wR_2 (all data)	0.1132	0.1805	0.1119

Table S2. Summary of important bond lengths (Å) and angles (°) from the crystallographically determined **1**.

Bond Lengths（Å）					
Os1-P1	2.2968(12)	Os1-Cl2	2.4222(12)	C3-O1	1.273(6)
Os1-P2	2.3318(12)	Os1-C1	1.913(5)	C2-P3	1.766(5)
Os1-O1	2.128(3)	C1-C2	1.434(7)	C3-C4	1.471(7)
Os1-Cl1	2.5359(12)	C2-C3	1.430(7)		
Bond Angles（º）					
C1-Os1-O1	78.03(17)	C1-C2-C3	112.5(4)	C3-O1-Os1	114.7(3)
Os1-C1-C2	117.6(4)	C2-C3-O1	116.3(4)		

Table S3. Summary of important bond lengths (Å) and angles (°) from the crystallographically determined **3**.

Bond Lengths（Å）					
Os1-P1	2.3547(14)	Os1-N2	2.138(5)	C3-O1	1.281(7)
Os1-P2	2.2773(14)	Os1-C1	1.951(5)	C2-P3	1.778(6)
Os1-O1	2.142(4)	C1-C2	1.406(8)	C3-C4	1.468(8)
Os1-N1	2.075(4)	C2-C3	1.436(8)		
Bond Angles（º）					
C1-Os1-O1	77.80(19)	C1-C2-C3	113.6(5)	C3-O1-Os1	114.4(3)
Os1-C1-C2	117.4(4)	C2-C3-O1	116.4(5)		

Table S4. Summary of important bond lengths (Å) and angles (°) from the crystallographically determined **4**.

Bond Lengths（Å）					
Os1-P1	2.2890(9)	Os1-Cl2	2.4550(8)	C3-O1	1.266(4)
Os1-P2	2.2534(8)	Os1-C1	1.935(3)	C2-P3	1.757(3)
Os1-O1	2.124(2)	C1-C2	1.421(4)	C3-C4	1.474(5)
Os1-Cl1	2.5149(8)	C2-C3	1.435(4)		
Bond Angles（º）					
C1-Os1-O1	78.78(11)	C1-C2-C3	113.3(3)	C3-O1-Os1	113.7(2)
Os1-C1-C2	116.2(2)	C2-C3-O1	117.0(3)		

2. Electrochemical data

Table S5. Electrochemical data for compounds **1** - **4** (1 mM in CH_2Cl_2) at 25 ºC in various supporting electrolyte systems.

Complex	^{n}-Bu_4NPF_6 (0.1 M)			^{n}-$Bu_4N[B(C_6F_5)_4]$ (0.05 M)		
	E_p^1 (V)	E_p^2 (V)	ΔE (V)	E_p^1 (V)	E_p^2 (V)	ΔE (V)
1	0.052	0.470	0.420	0.041	0.550	0.510
2	-0.004	0.516	0.520	-0.025	0.612	0.640
3	0.232	0.560	0.328	0.249	0.621	0.372
4	0.016	0.458	0.442	-0.004	0.523	0.530
5	0.172	0.724		0.143	0.704	
Fc	0.204			0.224		

[a] Peak potentials (E_p^1 and E_p^2) from square-wave voltammetry in 0.1 M CH_2Cl_2 at 10 Hz for SWV. Potentials E_p are in V vs Ag^+/Ag.

[b] Peak potential differences $\Delta E = E_p^2 - E_p^1$ are in V.

3. Molecular geometries

Table S6. Selected Bond Lengths(Å), Bond Angles(deg), and Dihedral Angles(deg) from the DFT-Optimized Structures **[1]**$^{n+}$ (n = 0, 1, 2) and crystal structure **1**.

	1	**[1]**	**[1]$^{1+}$**	**[1]$^{2+}$**
Bond Lengths (Å)				
Os1-P1	2.2968 (12)	2.43035	2.46117	2.50559
Os1-P2	2.3318 (12)	2.41788	2.49008	2.53164
Os1-Cl1	2.5359 (12)	2.59029	2.46749	2.41439
Os1-Cl2	2.4222 (12)	2.50882	2.49647	2.46215
Os1-C1	1.913 (5)	1.93523	1.97192	2.00416
Os1-O1	2.128 (3)	2.11157	2.07942	2.02115
C1-C2	1.434 (7)	1.43296	1.40085	1.38252
C2-C3	1.430 (7)	1.41797	1.43082	1.42893
C3- O1	1.273 (6)	1.30947	1.31406	1.33953
Bond Angles (deg)				
P1- Os1-P2	99.77 (4)	99.65760	102.25541	91.55710
Cl1- Os1- Cl2	84.21 (4)	87.08612	85.35250	82.53594
C1- Os1- O1	78.03 (17)	79.15768	77.04608	74.70604
Os1-C1- C2	117.6 (4)	114.81017	116.81790	118.47487
C1- C2- C3	112.5 (4)	114.89582	113.91130	112.67826
C2- C3- O1	116.3 (4)	115.22711	113.53295	110.97826
C3- O1- Os1	114.7 (3)	113.54355	116.68610	120.36923
Torsion Angles (deg)				
Os1-C1-C2-C3	-8.01	-11.10094	-9.37700	-10.25596
Os1-O1-C3-C2	5.97	11.32430	11.45623	14.51708
C2-C3-C4-C5	-23.99	-52.00509	-38.90370	-26.49110
O1-C3-C4-C5	162.30	132.01880	145.37038	158.00000

Table S7. Selected Bond Lengths(Å), Bond Angles(deg), and Dihedral Angles(deg) from the DFT-Optimized Structures **[2]**$^{n+}$ (n = 0, 1, 2)

	[2]	**[2]$^{1+}$**	**[2]$^{2+}$**
Bond Lengths (Å)			
Os1-P1	2.41919	2.45625	2.48470
Os1-P2	2.37777	2.46375	2.50160
Os1-O1	2.19015	2.06760	1.94008
Os1-O3	2.09146	2.10551	2.15261
Os1-C2	1.93450	1.96449	1.97309
Os1-O4	2.10339	2.08079	2.13427
O1-C1	1.36585	1.41032	1.46817
C1- O2	1.23002	1.21594	1.20476
C1- O3	1.39963	1.38229	1.34945
C2-C3	1.43367	1.40004	1.36180
C3-C4	1.42640	1.43653	1.46081
C4- O4	1.31237	1.31655	1.31273
Bond Angles (deg)			
P1- Os1-P2	98.71545	100.45718	103.14932
O1- Os1- O3	63.17645	64.84098	65.01666
C2- Os1- O4	79.94309	77.42606	73.90066
Os1-C2- C3	112.51144	115.49602	120.63194
C2- C3- C4	115.15529	113.82482	111.83144
C3- C4- O4	115.21190	113.65632	112.57449
C4- O4- Os1	111.79419	114.81994	116.17544
Os1-O1- C1	91.61495	94.32709	98.68463
O1-C1- O3	108.48944	106.49308	103.03084
C1- O3- Os1	94.87695	93.54699	93.20571
Torsion Angles (deg)			
Os1-O1-C1-O3	-12.09744	-8.08461	-2.32944
Os1-C2-C3-C4	-17.69374	-15.35031	-15.29674
Os1-O4-C4-C3	15.67985	16.55650	17.55425
C3-C4-C5-C6	-27.75776	-23.88684	-19.62320

O4-C4-C5-C6	157.80104	160.04752	165.50034

Table S8. Selected Bond Lengths(Å), Bond Angles(deg), and Dihedral Angles(deg) from the DFT-Optimized Structures **[3]**$^{n+}$ (n = 0, 1, 2) and crystal structure **3**.

	3	**[3]**	**[3]$^{1+}$**	**[3]$^{2+}$**
		Bond Lengths (Å)		
Os1-P1	2.3547 (14)	2.46079	2.48454	2.49516
Os1-P2	2.2773 (14)	2.40328	2.47419	2.48489
Os1-N1	2.075 (4)	2.04123	2.03908	2.02844
Os1-N2	2.138 (5)	2.11373	2.02883	1.98692
Os1-C1	1.951 (5)	1.96017	1.99329	2.03375
Os1-O1	2.142 (4)	2.12240	2.09488	2.05243
C1-C2	1.406 (8)	1.42697	1.40011	1.39193
C2-C3	1.436 (8)	1.42785	1.43937	1.45158
C3- O1	1.281 (7)	1.30615	1.30968	1.29027
C3-C4	1.468 (8)	1.46112	1.44689	1.44516
		Bond Angles (deg)		
P1- Os1-P2	98.81 (5)	99.54920	102.32179	100.59517
N1- Os1- N2	86.05 (18)	85.74083	85.43869	83.08441
C1- Os1- O1	77.80 (19)	78.96400	77.41331	74.53457
Os1-C1- C2	117.4 (4)	114.79358	115.75121	117.96591
C1- C2- C3	113.6 (5)	114.94655	114.22037	111.50931
C2- C3- O1	116.4 (5)	115.68500	114.43528	113.19667
C3- O1- Os1	114.4 (3)	113.53976	115.48720	120.09364
		Torsion Angles (deg)		
Os1-C1-C2-C3	-6.86	-9.29802	-10.01474	-8.40364
Os1-O1-C3-C2	1.47	11.60915	13.88008	15.61637
C2-C3-C4-C5	-24.75	-49.11874	-44.46051	-32.10078
O1-C3-C4-C5	161.43	135.33900	141.01277	153.20716

Table S9. Selected Bond Lengths(Å), Bond Angles(deg), and Dihedral Angles(deg) from the DFT-Optimized Structures **[4]**$^{n+}$ (n = 0, 1, 2) and crystal structure **4**.

	4	**[4]**	**[4]$^{1+}$**	**[4]$^{2+}$**
Bond Lengths (Å)				
Os1-P1	2.2890 (9)	2.39266	2.42344	2.49874
Os1-P2	2.2534 (8)	2.36893	2.45731	2.49287
Os1-Cl1	2.5149 (8)	2.53877	2.52425	2.47441
Os1-Cl2	2.4550 (8)	2.60475	2.47818	2.42060
Os1-C1	1.935 (3)	1.94429	1.98233	2.03123
Os1-O1	2.124 (2)	2.10425	2.07180	1.96003
C1-C2	1.421 (4)	1.43022	1.39495	1.39335
C2-C3	1.435 (4)	1.42615	1.44068	1.42985
C3- O1	1.266 (4)	1.30164	1.30609	1.35471
C3-C4	1.474 (5)	1.46316	1.44435	1.41726
Bond Angles (deg)				
P1- Os1-P2	93.53 (3)	94.12885	94.55050	89.43685
Cl1- Os1- Cl2	85.94 (3)	89.27048	88.84168	85.37883
C1- Os1- O1	78.78 (11)	79.15267	76.70400	75.80154
Os1-C1- C2	116.2 (2)	115.21203	117.39023	116.22909
C1- C2- C3	113.3 (3)	114.72880	113.60480	112.69483
C2- C3- O1	117.0 (3)	115.20082	113.19164	110.80572
C3- O1- Os1	113.7 (2)	114.47376	117.83578	120.65606
Torsion Angles (deg)				
Os1-C1-C2-C3	3.79	6.05316	4.66247	8.31706
Os1-O1-C3-C2	-9.97	-9.82997	-11.14620	-19.40070
C2-C3-C4-C5	-134.89	-142.71514	-153.88473	-165.50079
O1-C3-C4-C5	40.35	34.07838	23.19668	12.38937

Table S10. Energy and composition of frontier molecular orbitals in the complex **1**

MO		eV	Cl1	$(PPh_3)1$	Os	$(PPh_3)2$	Cl2	C=C-C=O	$(PPh_3)3$	C_5H_4	Fe	C_5H_5
292	L+3	-1.08	0	0	1	0	0	3	96	0	0	0
291	L+2	-1.23	1	0	15	1	1	37	33	4	6	2
290	L+1	-1.36	0	0	0	0	0	3	97	0	0	0
289	LUMO	-1.53	0	0	2	0	0	7	90	0	1	0
288	HOMO	-4.24	23	6	64	0	1	6	0	0	0	0
287	H-1	-4.52	10	4	56	2	15	11	2	0	0	0
286	H-2	-4.79	17	0	33	2	12	13	0	4	17	2
285	H-3	-5.03	0	0	0	0	0	0	0	7	88	5

Table S11. Energy and composition of frontier molecular orbitals in the complex $\mathbf{1}^+$

MO		eV	Cl1	$(PPh_3)1$	Os	$(PPh_3)2$	Cl2	C=C-C=O	$(PPh_3)3$	C_5H_4	Fe	C_5H_5
292α	α-LUSO+3	-3.34	0	14	32	20	7	6	21	0	0	0
1122β	β-LUSO+3	-3.60	0	0	0	0	0	4	96	0	0	0
291α	α-LUSO+2	-3.60	0	0	0	0	0	3	97	0	0	0
1121β	β-LUSO+2	-3.70	0	0	1	0	0	3	95	0	1	0
290α	α-LUSO+1	-3.70	0	0	1	0	0	3	95	0	1	0
1120β	β-LUSO+1	-4.34	1	0	17	1	2	60	3	6	7	3
289α	α-LUSO	-4.37	1	0	13	1	2	64	2	7	7	3
1119β	β-LUSO	-5.58	15	5	72	0	1	7	0	0	0	0
288α	α-HOSO	-7.48	0	0	2	0	0	2	0	7	83	6
1118β	β-HOSO	-7.49	1	0	4	0	1	2	0	7	81	4
287α	α-HOSO-1	-7.54	0	0	0	0	0	0	0	6	88	6
1117β	β-HOSO-1	-7.55	0	0	0	0	0	0	0	6	88	6
286α	α-HOSO-2	-8.02	9	2	44	2	32	9	1	0	1	0
1116β	β-HOSO-2	-7.78	9	5	49	2	24	10	1	0	0	0
285α	α-HOSO-3	-8.11	21	6	29	4	17	7	0	7	2	7
1115β	β-HOSO-3	-7.96	16	0	33	3	16	11	0	8	6	7

Table S12. Energy and composition of frontier molecular orbitals in the complex **2**

MO		eV	$(PPh_3)1$	Os	$(PPh_3)2$	$\eta2\text{-}CO_3$	C=C-C=O	$(PPh_3)3$	C_5H_4	Fe	C_5H_5
290	L+3	-0.98	0	1	0	0	3	95	0	1	0
289	L+2	-1.09	0	8	3	1	25	53	3	6	1
288	L+1	-1.21	0	4	1	0	16	72	2	4	1
287	LUMO	-1.42	0	2	0	0	5	90	1	1	1
286	HOMO	-4.10	5	67	2	18	8	0	0	0	0
285	H-1	-4.44	6	63	4	20	5	0	1	1	0
284	H-2	-4.76	0	36	4	10	22	3	3	21	1
283	H-3	-5.02	0	0	0	0	0	0	6	87	7

Table S13. Energy and composition of frontier molecular orbitals in the complex $\mathbf{2}^+$

MO		eV	$(PPh_3)1$	Os	$(PPh_3)2$	$\eta2\text{-}CO_3$	C=C-C=O	$(PPh_3)3$	C_5H_4	Fe	C_5H_5
290α	α-LUSO+3	-3.23	0	1	0	0	2	96	0	1	0
1130β	β-LUSO+3	-3.47	0	0	0	0	4	96	0	0	0
289α	α-LUSO+2	-3.47	0	0	0	0	4	96	0	0	0
1129β	β-LUSO+2	-3.62	0	1	0	0	3	95	0	1	0
288α	α-LUSO+1	-3.62	0	1	0	0	3	95	0	1	0
1128β	β-LUSO+1	-4.19	0	15	1	2	58	4	7	9	4
287α	α-LUSO	-4.22	0	12	2	2	60	4	7	9	4
1127β	β-LUSO	-5.34	5	68	1	17	9	0	0	0	0
286α	α-HOSO	-7.42	0	3	0	1	2	0	7	81	6
1126β	β-HOSO	-7.43	0	6	0	2	2	0	6	78	6
285α	α-HOSO-1	-7.49	0	0	0	0	0	0	5	88	7
1125β	β-HOSO-1	-7.50	0	0	0	0	0	0	5	88	7
284α	α-HOSO-2	-7.98	4	50	3	29	7	0	3	2	2
1124β	β-HOSO-2	-7.79	4	60	4	22	4	1	1	2	2
283α	α-HOSO-3	-8.11	6	54	1	25	11	0	1	1	1
1123β	β-HOSO-3	-7.95	1	38	4	10	20	2	11	9	5

Table S14. Energy and composition of frontier molecular orbitals in the complex **3**

MO		eV	NCS1	$(PPh_3)1$	Os	$(PPh_3)2$	NCS2	C=C-C=O	$(PPh_3)3$	C_5H_4	Fe	C_5H_5
304	L+3	-1.22	0	0	1	0	0	2	97	0	0	0
303	L+2	-1.43	2	1	9	2	1	32	46	3	3	1
302	L+1	-1.52	0	0	1	0	0	5	92	1	1	0
301	LUMO	-1.69	2	0	6	2	0	22	65	1	2	0
300	HOMO	-4.13	68	2	27	0	0	2	0	0	1	0
299	H-1	-4..35	70	0	13	0	7	9	1	0	0	0
298	H-2	-4.63	12	1	25	2	57	1	0	1	1	0
297	H-3	-4.84	11	0	11	1	69	4	0	1	3	0

Table S15. Energy and composition of frontier molecular orbitals in the complex $\mathbf{3}^{+}$

MO		eV	NCS1	$(PPh_3)1$	Os	$(PPh_3)2$	NCS2	C=C-C=O	$(PPh_3)3$	C_5H_4	Fe	C_5H_5
304α	α-LUSO+3	-3.28	0	0	1	0	0	3	95	0	1	0
1170β	β-LUSO+3	-3.60	0	0	0	0	0	3	97	0	0	0
303α	α-LUSO+2	-3.60	0	0	0	0	0	3	97	0	0	0
1169β	β-LUSO+2	-3.66	0	0	1	0	0	4	94	0	1	0
302α	α-LUSO+1	-3.66	0	0	1	0	0	4	94	0	1	0
1168β	β-LUSO+1	-4.43	3	1	14	2	1	65	2	6	5	1
301α	α-LUSO	-4.44	3	1	12	2	1	66	2	6	6	1
1167β	β-LUSO	-5.87	33	4	53	0	4	6	0	0	0	0
300α	α-HOSO	-7.33	0	0	10	0	54	1	0	3	29	3
1166β	β-HOSO	-7.22	8	0	17	1	69	2	0	0	2	1
299α	α-HOSO-1	-7.34	3	0	8	0	40	2	0	3	42	2
1165β	β-HOSO-1	-7.30	4	0	10	0	37	4	0	4	39	2
298α	α-HOSO-2	-7.41	0	0	1	0	6	0	0	5	82	6
1164β	β-HOSO-2	-7.41	1	0	1	0	4	0	0	6	84	4
297α	α-HOSO-3	-7.45	2	0	5	0	63	4	0	1	22	3
1163β	β-HOSO-3	-7.43	0	0	3	0	35	2	60	0	0	0

Table S16. Energy and composition of frontier molecular orbitals in the complex **4**

MO		eV	Cl1	(PPh_2-C_2H_4)1	Os	(PPh_2-C_2H_4)2	Cl2	C=C-C=O	PPh_3	C_5H_4	Fe	C_5H_5
267	L+3	-1.03	0	0	3	0	0	7	89	0	1	0
266	L+2	-1.12	0	0	8	0	1	28	55	3	4	1
265	L+1	-1.31	0	0	6	0	1	20	68	2	2	1
264	LUMO	-1.39	0	0	0	0	0	0	100	0	0	0
263	HOMO	-4.23	20	6	66	0	0	8	0	0	0	0
262	H-1	-4.46	8	2	60	5	13	11	1	0	0	0
261	H-2	-4.80	8	1	38	2	14	12	0	3	19	3
260	H-3	-5.02	0	0	0	0	0	0	0	6	88	6

Table S17. Energy and composition of frontier molecular orbitals in the complex $\mathbf{4}^{+}$

MO		eV	Cl1	(PPh_3-C_2H_4)1	Os	(PPh_3-C_2H_4)2	Cl2	C=C-C=O	PPh_3	C_5H_4	Fe	C_5H_5
267α	α-LUSO+3	-3.29	0	0	1	0	0	2	97	0	0	0
1021β	β-LUSO+3	-3.53	0	0	0	0	0	4	96	0	0	0
266α	α-LUSO+2	-3.54	0	0	0	0	0	4	96	0	0	0
1020β	β-LUSO+2	-3.65	0	0	0	0	0	1	99	0	0	0
265α	α-LUSO+1	-3.65	0	0	0	0	0	2	98	0	0	0
1019β	β-LUSO+1	-4.30	1	0	15	1	2	63	0	6	7	5
264α	α-LUSO	-4.32	1	0	12	1	2	66	0	6	8	4
1018β	β-LUSO	-5.68	13	5	74	0	0	8	0	0	0	0
263α	α-HOSO	-7.45	0	0	2	0	0	2	0	7	83	6
1017β	β-HOSO	-7.46	0	0	4	0	1	2	0	7	82	4
262α	α-HOSO-1	-7.51	0	0	0	0	0	0	0	6	88	6
1016β	β-HOSO-1	-7.51	0	0	0	0	0	0	0	6	88	6
261α	α-HOSO-2	-8.01	10	3	47	3	29	7	0	0	1	0
1015β	β-HOSO-2	-7.78	11	2	54	3	21	8	0	0	1	0
260α	α-HOSO-3	-8.15	8	5	31	1	31	6	1	8	2	7
1014β	β-HOSO-3	-7.98	7	3	36	2	25	8	0	8	5	6

Table S18. Major electronic excitations for compounds [1] and $[1]^+$, as determined by using TDDFT methods (B3LYP/6-31G*)

Compound	λ [nm]	f	Major contributions ([%])	Assignment
[1]	684.8	0.002	HOMO-3→LUMO+15(24)	M(Fe)→L(PPh_3)CT
	540.3	0.005	HOMO→LUMO(63)	M(Os)L(Cl1)→L(PPh_3^+)CT
			HOMO→LUMO+2(27)	M(Os)L(Cl1)→LCT
	538.2	0.002	HOMO-3→LUMO+13(13)	M(Fe)→LCT
	459.8	0.014	HOMO-2→LUMO(79)	M(Os)→L(PPh_3^+)CT
$[1]^+$	704.76	0.009	α-HOSO→α-LUSO(16)	M(Fe)→ L(C=C-C=O)CT
			β-HOSO→β-LUSO+1 (14)	M(Fe)→L(C=C-C=O)CT

Table S19. Major electronic excitations for compounds [2] and $[2]^+$.

Compound	λ [nm]	f	Major contributions ([%])	Assignment
[2]	698.9	0.004	HOMO-3→LUMO+15(19)	M(Fe)→LCT
	549.7	0.006	HOMO-3→LUMO+15(14)	M(Fe)→LCT
			HOMO-1→LUMO(15)	M(Os)L(η^2-CO_3)→L(PPh_3^+)CT
			HOMO-1→LUMO+2(16)	M(Os)L(η^2-CO_3)→L(PPh_3^+)CT
	544.6	0.005	HOMO→LUMO(62)	M(Os)L(η^2-CO_3)→L(PPh_3^+)CT
	454.7	0.016	HOMO-2→LUMO(94)	M(Os)→L(PPh_3^+)CT
$[2]^+$	719.4	0.010	α-HOSO→α-LUSO (17)	M(Fe)→ L(C=C-C=O)CT
			β-HOSO→β-LUSO+1 (15)	M(Fe)→ L(C=C-C=O)CT

Table S20. Major electronic excitations for compounds [3] and $[3]^+$.

Compound	λ [nm]	f	Major contributions ([%])	Assignment
[3]	691.7	0.002	HOMO-5→LUMO+16(25)	M(Fe)→LCT
	588.5	0.007	HOMO-2→LUMO(26)	M(Os)L(NCS2)→L(PPh_3^+)CT
			HOMO-1→LUMO(45)	M(Os)L(NCS1)→L(PPh_3^+)CT
	546.3	0.009	HOMO-4→LUMO+16(19)	M(Fe)→LCT
	531.4	0.012	HOMO-2→LUMO(21)	M(Os)L(NCS2)→L(PPh_3^+)CT
			HOMO-1→LUMO(40)	M(Os)L(NCS1)→L(PPh_3^+)CT
	504.1	0.018	HOMO-1→LUMO+1(68)	M(Os)L(NCS1)→L(PPh_3^+)CT
	494.8	0.027	HOMO-1→LUMO+1(21)	M(Os)L(NCS1)→L(PPh_3^+)CT
			HOMO-1→LUMO+2(62)	M(Os)L(NCS1)→LCT
$[3]^+$	822.0	0.004	β-HOSO-9→β-LUSO (41)	L→M(Os)L(NCS1)CT
			β-HOSO-6→β-LUSO (22)	L→M(Os)L(NCS1)CT
	731.1	0.022	α-HOSO→α-LUSO (14)	L(NCS2)→L(C=C-C=O)CT
				M(Fe)→L(C=C-C=O)CT
			β-HOSO-5→β-LUSO(18)	L(NCS1)→M(Os)CT

Table S21. Major electronic excitations for compounds [4] and $[4]^+$.

Compound	λ [nm]	f	Major contributions ([%])	Assignment
[4]	680.4	0.002	HOMO-3→LUMO+12(36)	M(Fe)→LCT
	536.5	0.002	HOMO-3→LUMO+12(29)	M(Fe)→LCT
	481.9	0.005	HOMO-1→LUMO(98)	M(Os)→L(PPh_3)CT
	438.1	0.007	HOMO-2→LUMO(88)	M(Os)→L(PPh_3)CT
$[4]^+$	705.5	0.008	α-HOSO→α-LUSO (18)	M(Fe)→L(C=C-C=O)CT
			β-HOSO→β-LUSO+1 (16)	M(Fe)→L(C=C-C=O)CT

4. NMR data

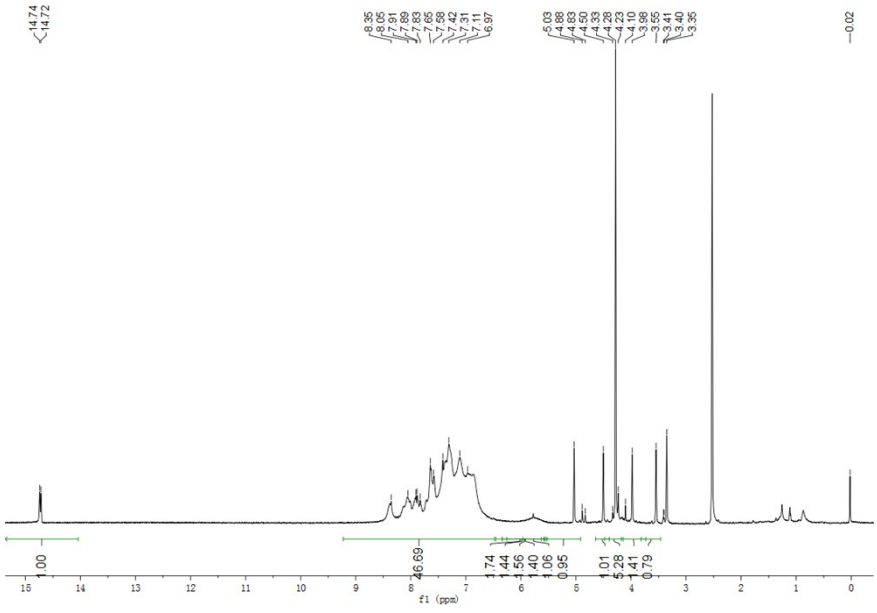

(**a**)

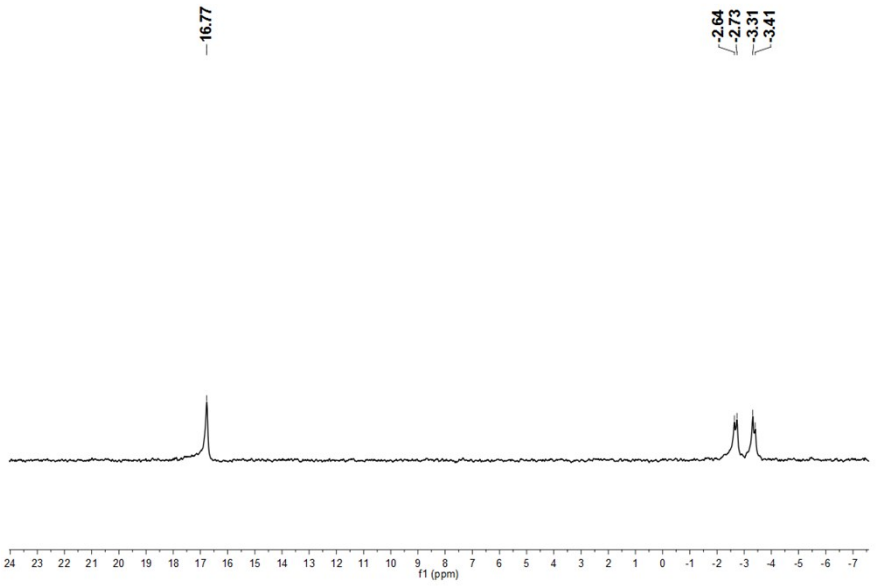

(**b**)

Figure S1 ^{1}H NMR (D6-DMSO, 500 MHz) (**a**) and $^{31}P\{^{1}H\}$ NMR (D6-DMSO, 202.47 MHz) (**b**) for complex **1**.

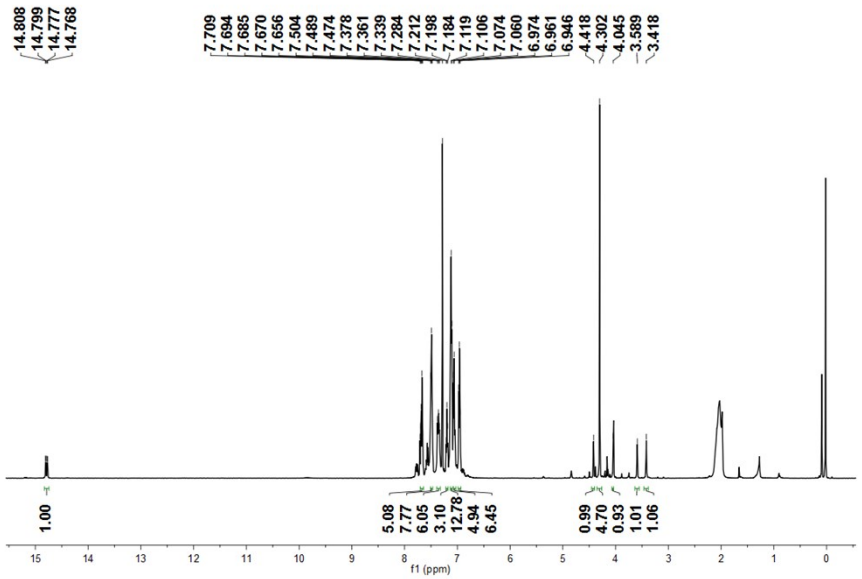
14.808
14.799
14.777
14.768
7.709
7.694
7.685
7.670
7.656
7.504
7.489
7.474
7.378
7.361
7.339
7.284
7.212
7.198
7.184
7.119
7.106
7.074
7.060
6.974
6.961
6.946
4.418
4.302
4.045
3.589
3.418
1.00
5.08
7.77
6.05
3.10
12.78
4.94
6.45
0.99
4.70
0.93
1.01
1.06
f1 (ppm)

(**a**)

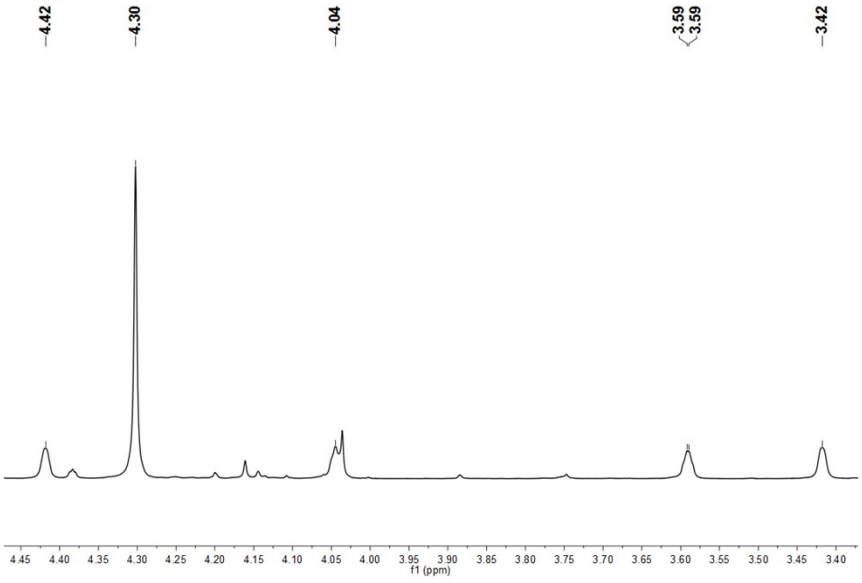
4.42
4.30
4.04
3.59
3.59
3.42
f1 (ppm)

(**b**)

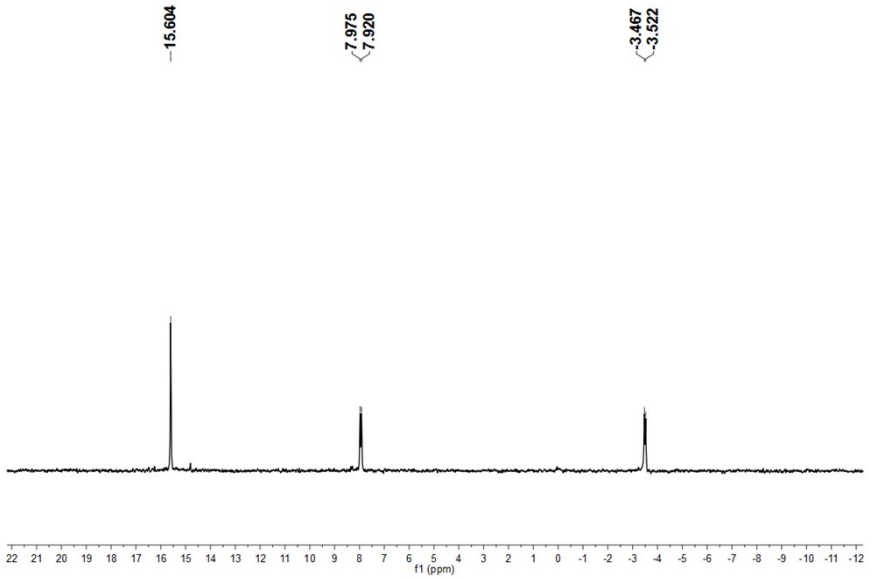

(**c**)

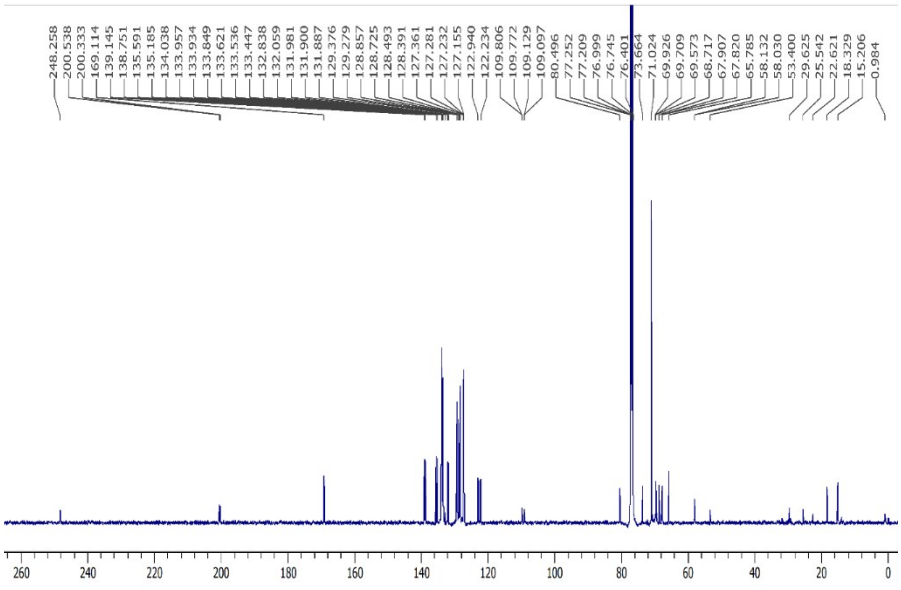

(**d**)

Figure S2 ^{1}H NMR ($CDCl_3$, 500 MHz) (**a**, **b**), $^{31}P\{^{1}H\}$ NMR ($CDCl_3$, 202.47 MHz) (**c**), and $^{13}C\{^{1}H\}$ NMR ($CDCl_3$, 125.77 MHz) (**d**) of complex **2**.

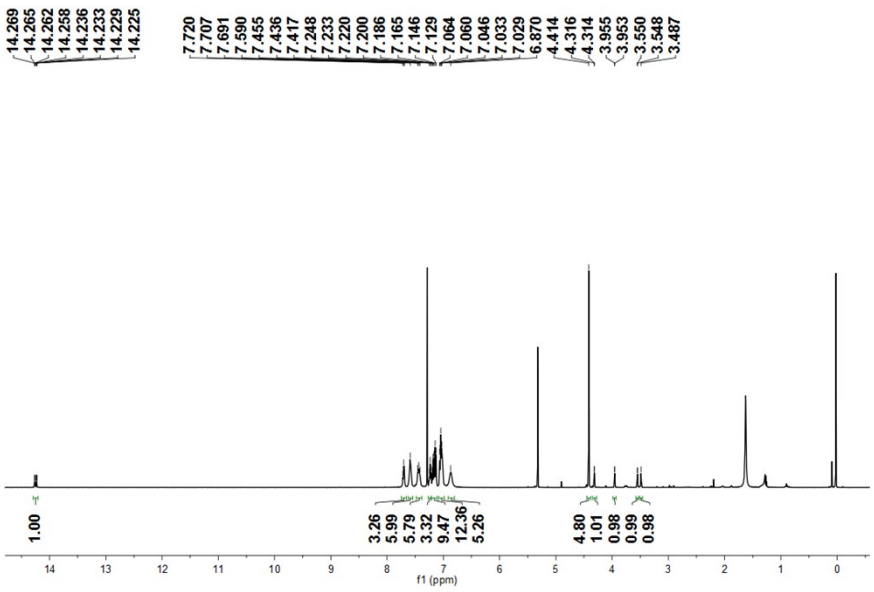
14.269
14.265
14.262
14.258
14.236
14.233
14.229
14.225
7.720
7.707
7.691
7.590
7.455
7.436
7.417
7.248
7.233
7.220
7.200
7.186
7.165
7.146
7.129
7.064
7.060
7.046
7.033
7.029
6.870
4.414
4.316
4.314
3.955
3.953
3.550
3.548
3.487
1.00
3.26
5.99
5.79
3.32
9.47
12.36
5.26
4.80
1.01
0.98
0.99
0.98
f1 (ppm)

(**a**)

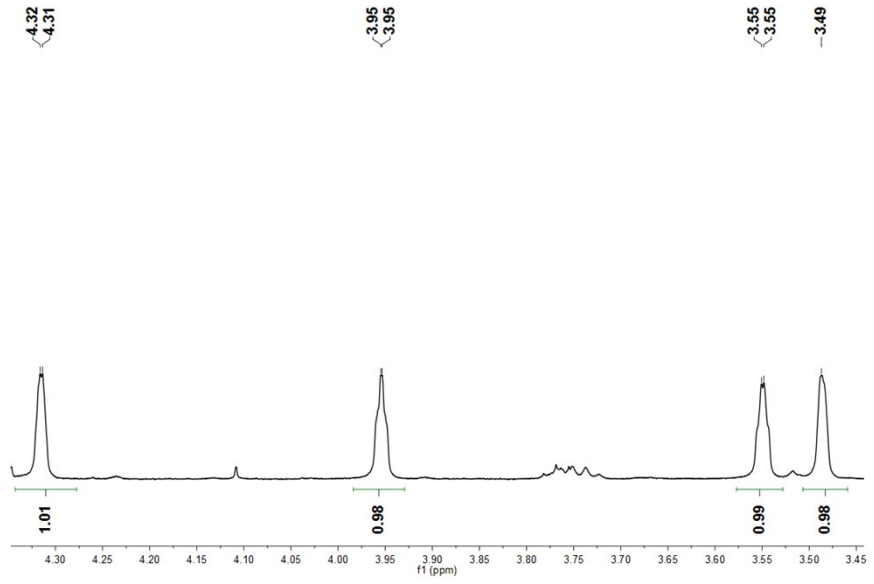
4.32
4.31
3.95
3.95
3.55
3.55
3.49
1.01
0.98
0.99
0.98
f1 (ppm)

(**b**)

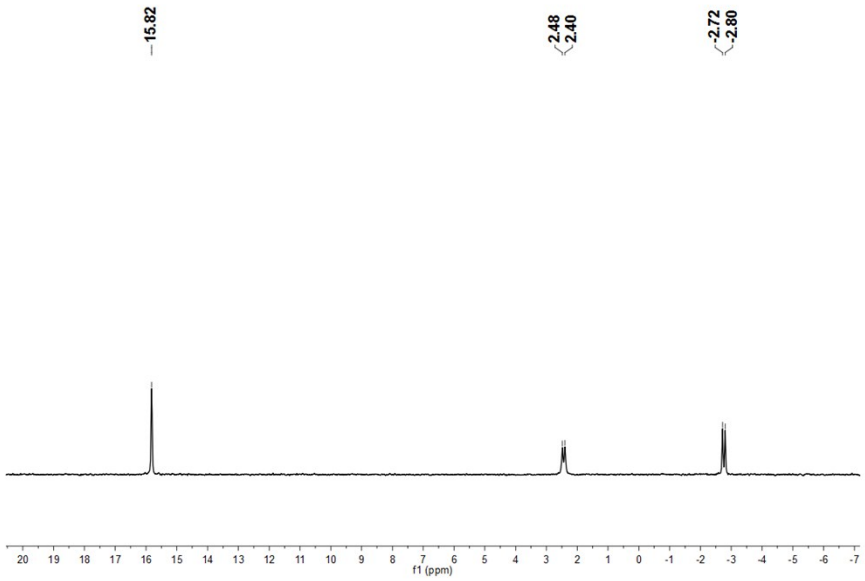

(**c**)

Figure S3 ^{1}H NMR ($CDCl_3$, 500 MHz) (**a** and **b**) and $^{31}P\{^{1}H\}$ NMR ($CDCl_3$, 202.47 MHz) (**c**) of complex **3**.

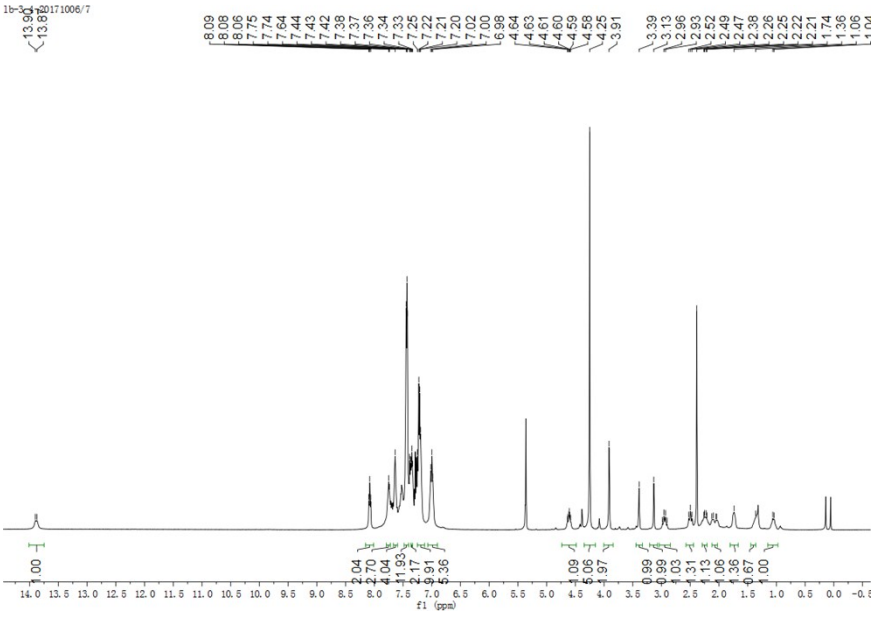

(**a**) ^{1}H NMR (CD_2Cl_2, 500 MHz).

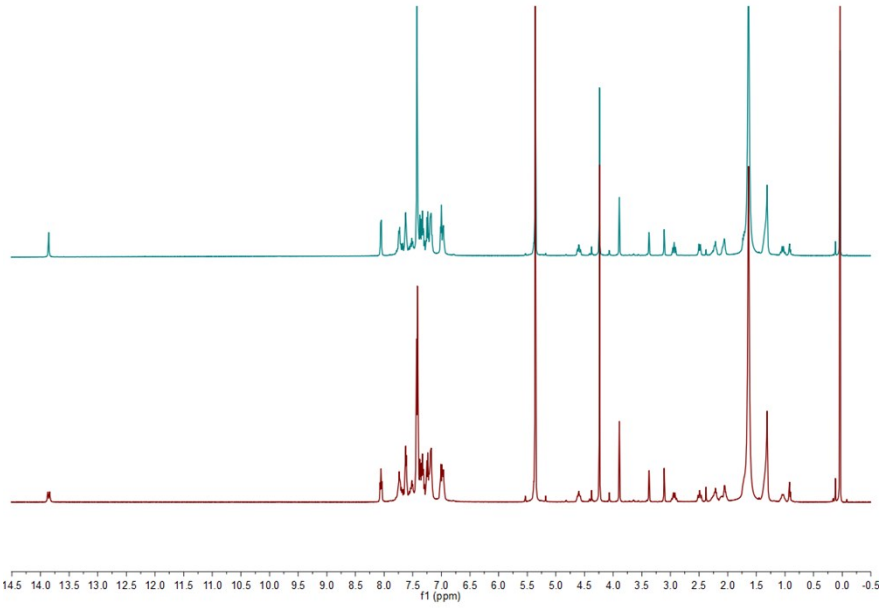

(**b**) ^{1}H(CD_2Cl_2, 500 MHz) NMR (up) and $^{1}H\{^{31}P\}$ NMR (down).

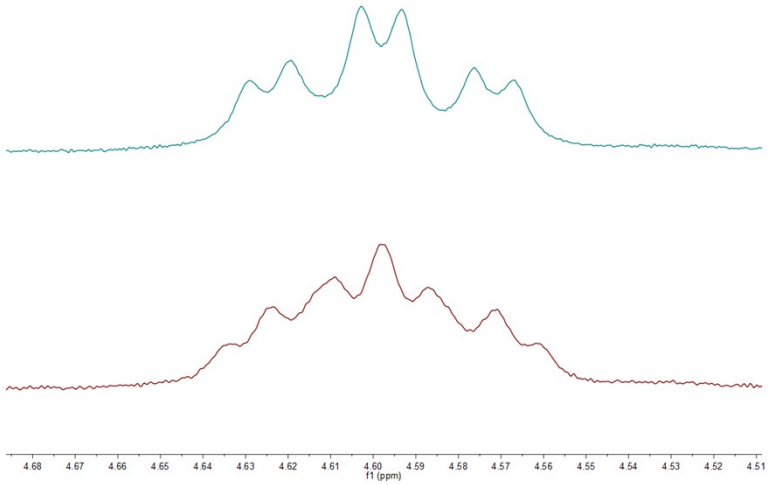

(**c**) $^{1}H(CD_2Cl_2$, 500 MHz) NMR (up) and $^{1}H\{^{31}P\}$ NMR (down) of the peak at 4.60 ppm.

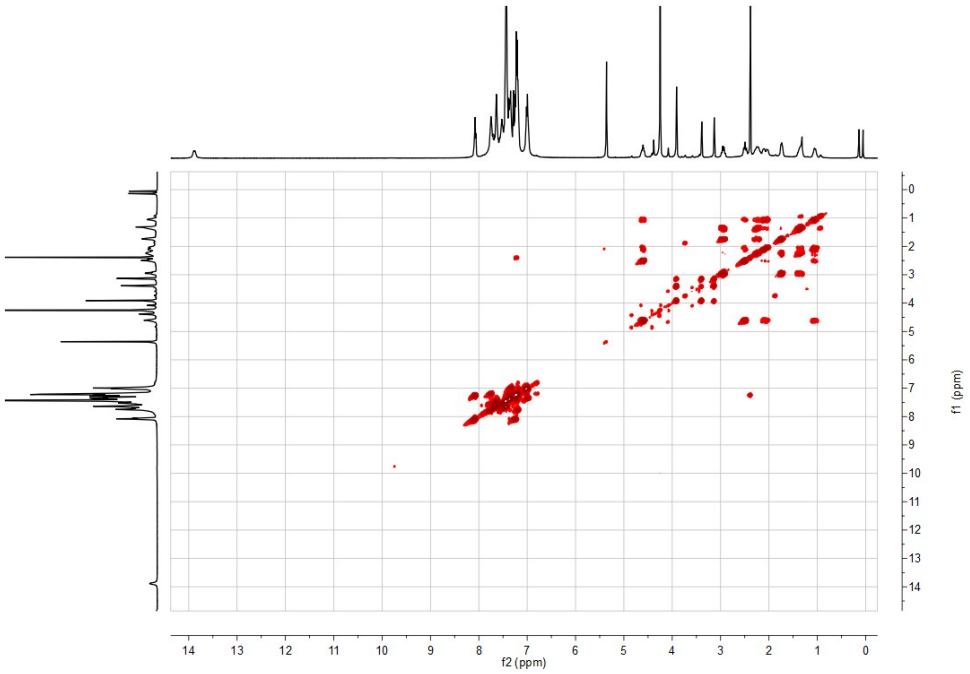

(**d**) H-H COSY

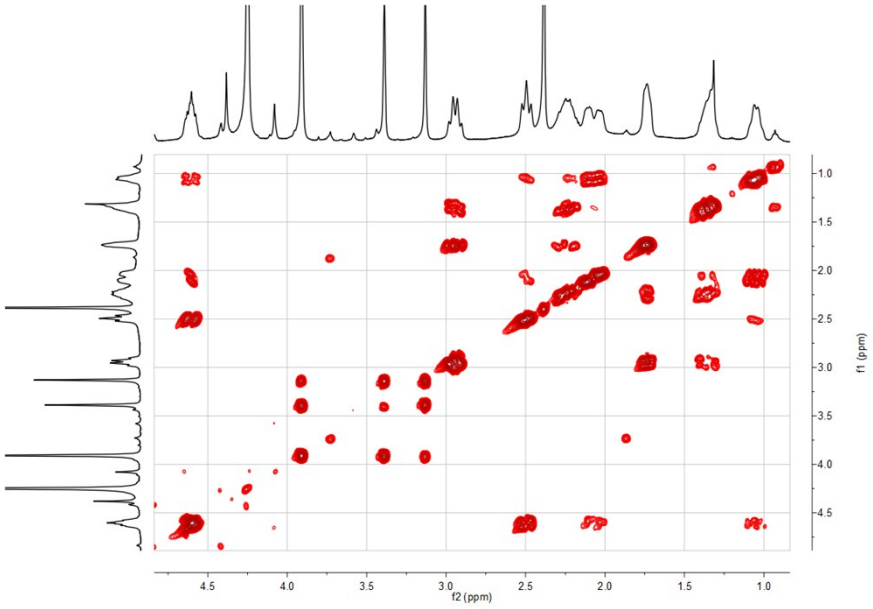

(**e**) H-H COSY (1.0 ppm-4.7 ppm)

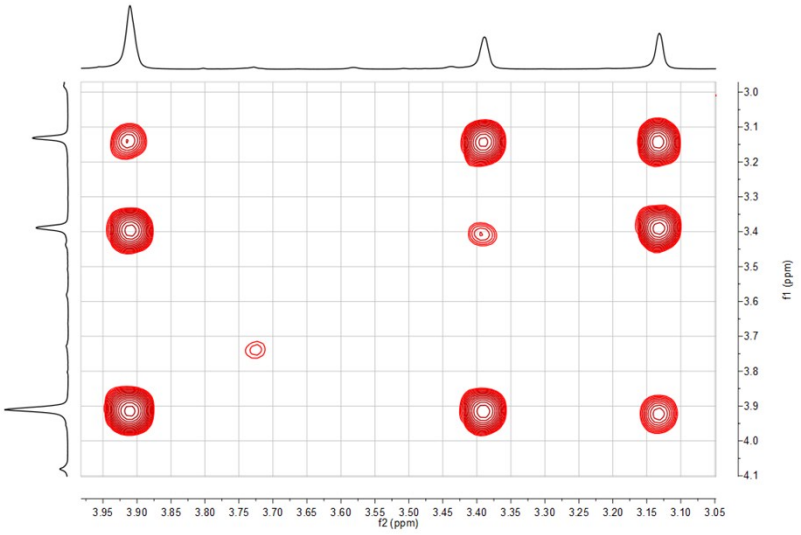

(**f**) H-H COSY (3.0 ppm-4.1 ppm)

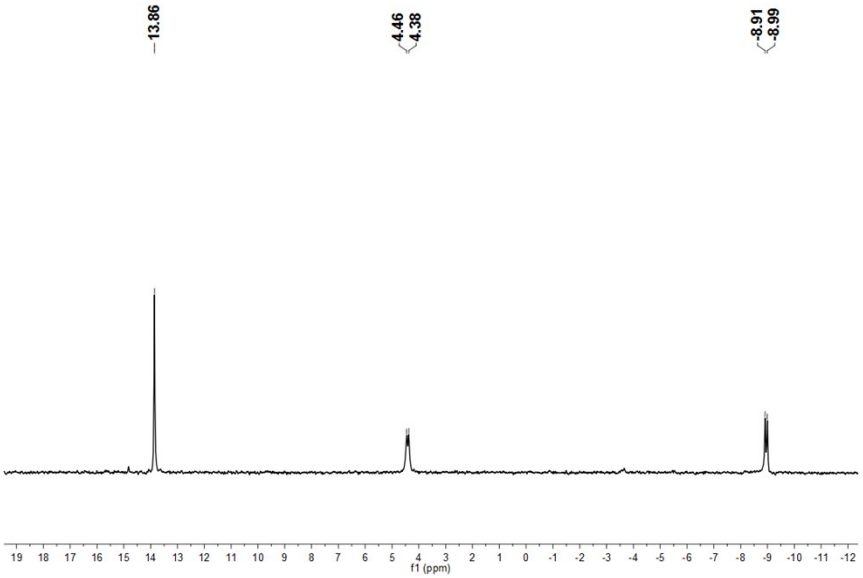

(**g**) $^{31}P\{^{1}H\}$ (CD_2Cl_2, 125 MHz)

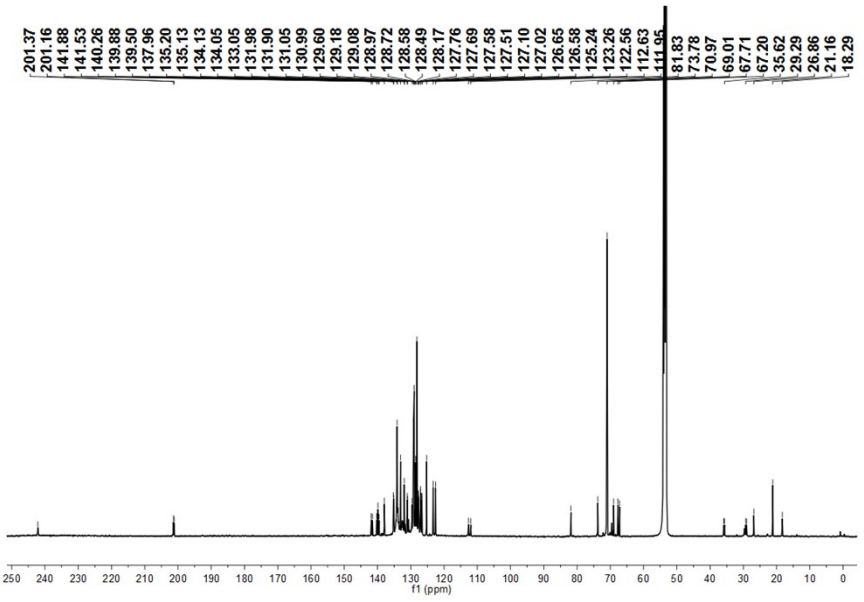

(**h**) $^{13}C\{^{1}H\}$ NMR (CD_2Cl_2, 125 MHz)

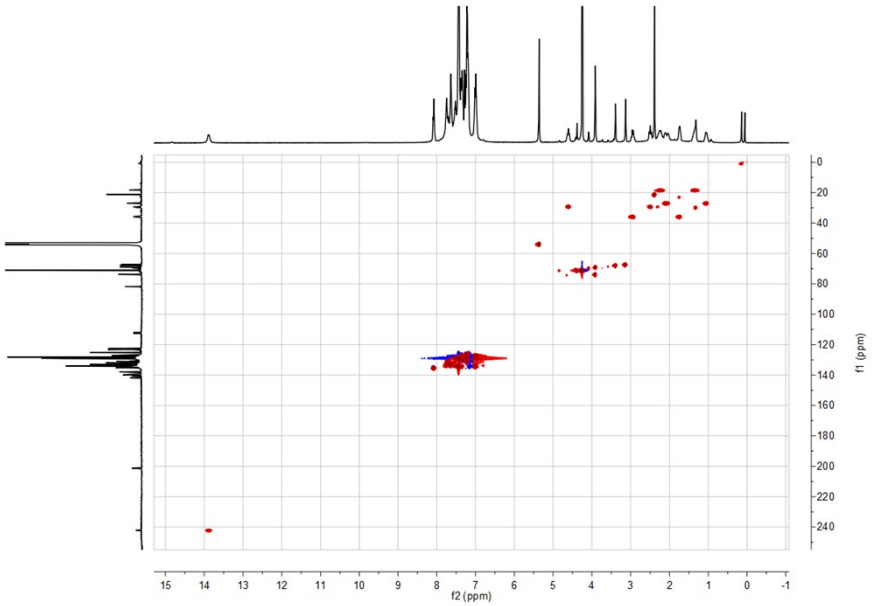

(**i**) C-H COSY

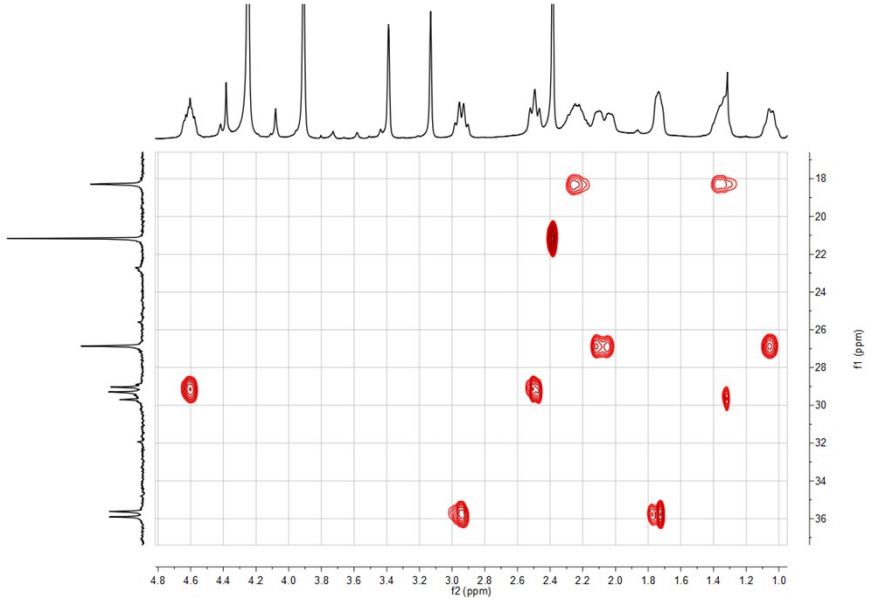

(**j**) C-H COSY ($^{13}C\{^{1}H\}$: 18-36 ppm, ^{1}H: 1.0-4.8 ppm)

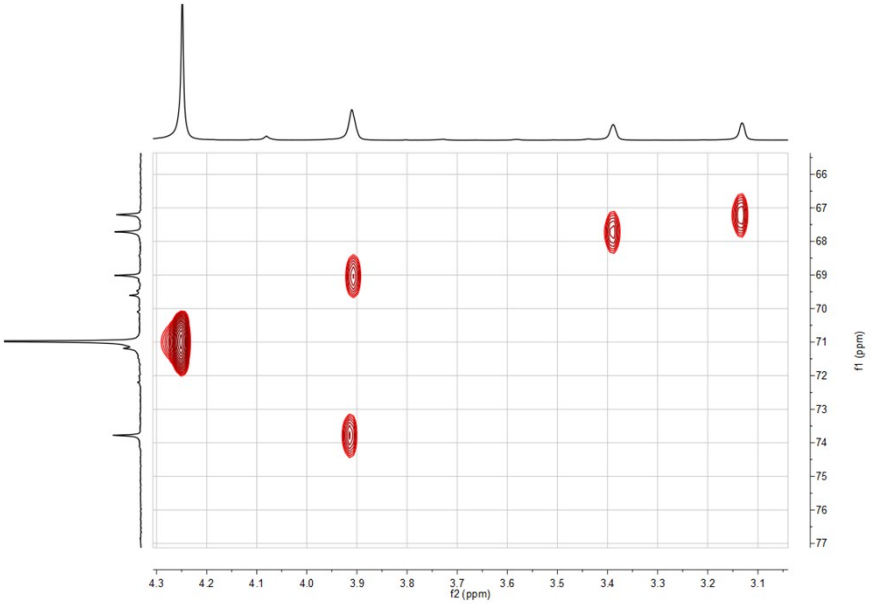

(**k**) C-H COSY ($^{13}C\{^{1}H\}$: 66-77 ppm, ^{1}H: 3.1-4.3 ppm)

Figure S4 NMR spectra of complex **4** (**a**-**k**)